

On the Second-order Statistics of the Channel Parameters for BFDM/OQAM Systems

Bayarpurev Mongol, Takaya Yamazato, Hiraku Okada, Masaaki Katayama

Graduate School of Engineering, Nagoya University

Furo-cho Chikusa-ku Nagoya-shi, Aichi-ken, 464-8603, JAPAN

Tel/Fax: +81-52-789-2729/ +81-52-789-3173

E-mail: mongol@katayama.nuee.nagoya-u.ac.jp, {yamazato,okada,katayama}@nuee.nagoya-u.ac.jp

Abstract—Recently, there has been increased interest in using multicarrier systems in rapidly time-varying multipath environment. Biorthogonal Frequency Division Multiplexing based on Offset QAM (BFDM/OQAM) is an attractive modulation method since it allows time-frequency well-localized pulses even at critical sampling (i.e. maximum spectral efficiency). BFDM/OQAM system is naturally strong against intersymbol and intercarrier interference (ISI/ICI). However, for further improvement of the system a study on the channel statistics is needed. In this paper we analytically examine the channel parameters for BFDM/OQAM and derive their second-order statistics.

I. INTRODUCTION

Orthogonal Frequency Division Multiplexing (OFDM) signal is known to be robust against frequency selectivity, caused by multipath channels. However, it is relatively sensitive to time selectivity, caused by rapid variation of the mobile channels. These dispersive time-varying channels result in intersymbol and intercarrier interference (ISI/ICI)[1].

By introducing pulse shaping filter, it is possible to reduce the ISI/ICI and increase carrier frequency offset robustness [2]. The performance of such pulse-shaping OFDM system in dispersive time-varying channels depends critically on the time-frequency localization of the transmitter and receiver filters. Ideally, the system should use time-frequency well-localized transmitter pulse while keeping maximal spectral efficiency. Spectral efficiency ρ of the OFDM system may be approximated by $\rho = 1/(TF)$ symbols per second per Hertz, here T is symbol period and F is subcarrier separation. It is obvious that maximal spectral efficiency is $\rho_{max} = 1$. However, due to Balian-Low theorem [3], it is impossible for the OFDM system, based on Quadrature Amplitude Modulation (QAM) to have the well-localized pulses at maximal spectral efficiency [4]. Number of interesting pulse-shaping OFDM systems are proposed recently to deal with the problem. Orthogonal Frequency Division Multiplexing and Biorthogonal Frequency Division Multiplexing systems based on Offset QAM (OFDM/OQAM and BFDM/OQAM), allow construction of well-localized pulses at critical sampling, which is desirable in high data-rate applications [5]. Moreover, the second also allows construction of Gaussian pulse, which has the best TFL. A use of time-frequency well-localized transmitter pulses for BFDM/OQAM systems results in decrease in ISI/ICI and in some practical cases it may be neglected [6]. However in rapidly time-varying multipath channels careful

investigation of ISI/ICI and proper equalization is needed for further improvement for the systems. Statistical analysis of the channel parameters are essential for construction of robust channel estimation and equalization.

In this paper we analyze ISI/ICI for BFDM/OQAM systems in time-frequency dispersive environment, analytically derive second-order statistics for the channel parameters and numerically evaluate them for the case when Gaussian pulse is employed. To simulate the BFDM/OQAM system we construct Gaussian transmitter pulse and receiver pulse that biorthogonal to the transmitter pulse. We show how channel parameter statistics depend on the channel condition parameters such as maximum Doppler shift, root-mean-square (rms) delay spread.

II. MOBILE MULTIPATH CHANNEL

Consider a linear multipath propagation channel characterized by a infinite set of paths with complex amplitudes $\{h_m\}$, delays $\{\tau_m\}$, incident angles $\{\theta_m\}$ with respect to direction of mobile station motion. We make standard assumption wide-sense stationary uncorrelated scattering (WSSUS). Further we assume Rayleigh paths with exponentially decaying delay profile with root-mean-square delay spread τ_0 :

$$\sum_{m:\tau_m \in (\tau, \tau + d\tau)} \mathbf{E}\{|h_m|^2\} = \frac{1}{\tau_0} e^{-\tau/\tau_0} d\tau \quad (1)$$

where $\mathbf{E}\{\cdot\}$ is expectation, τ_0 is root mean square delay spread, τ_m and h_m are respectively, the delay and complex amplitude of the m -th path. In this paper make the following assumption.

Assumption 1: For arbitrary interval $[\tau; \tau + d\tau]$ there exist paths such that delays of the paths belong to this interval.

If we denote sum of the complex amplitudes of the paths in *Assumption 1:* with $h(\tau)$ then WSSUS implies that:

$$\mathbf{E}\{h(\tau_1)h^*(\tau_2)\} = \frac{1}{\tau_0} e^{-\tau/\tau_0} \delta(\tau_1 - \tau_2) \quad (2)$$

We also assume that the channel has Jakes' Doppler power spectrum. From [7], time variation (i.e. flat fading) of $h(\tau)$ can be expressed as:

$$\begin{aligned}\xi(t) &= \xi_c(t) + j\xi_s(t) \\ \xi_c(t) &= \sqrt{\frac{2}{m_\tau}} \sum_{m:\tau_m \in (\tau, \tau+d\tau)} \cos(2\pi f_d t \cos \theta_m + \phi_m) \\ \xi_s(t) &= \sqrt{\frac{2}{m_\tau}} \sum_{m:\tau_m \in (\tau, \tau+d\tau)} \sin(2\pi f_d t \cos \theta_m + \phi_m)\end{aligned}\quad (3)$$

where, θ_i and ϕ_i are respectively, arrival angle and phase shift of the i -th path, f_d is maximum Doppler shift, m_τ is the number of paths with delays belong to the interval $[\tau_m \in (\tau, \tau + d\tau)]$. Autocorrelation and crosscorrelation functions of this normalized fading process are given by [7]:

$$\begin{aligned}R_{\xi_c \xi_c}(\Delta t) &= \mathbf{E}\{\xi_c(t + \Delta t)\xi_s(t)\} = J_0(2\pi f_d \Delta t) \\ R_{\xi_s \xi_s}(\Delta t) &= \mathbf{E}\{\xi_s(t + \Delta t)\xi_s(t)\} = J_0(2\pi f_d \Delta t) \\ R_{\xi_s \xi_c}(\Delta t) &= R_{\xi_c \xi_s}(\Delta t) = 0\end{aligned}\quad (4)$$

where, $J_0(\cdot)$ is 0-order Bessel function of the first kind.

III. BFDMM/OQAM SYSTEM, ISI/ICI AND CHANNEL PARAMETERS

Here, we review some mathematical background for BFDMM/OQAM, analyze the ISI/ICI for the system, that occur in the channel described in Section II, and derive second-order statistics for the channel parameters.

A. BIORTHOGONAL BASIS

Let us briefly review the mathematical basics of BFDMM/OQAM system. Define set \mathbf{G} , consists of the pairs of translations and modulations of a real transmitter pulse shape $g(t)$:

$$\mathbf{G} = \begin{cases} g_{k,l}^{\mathcal{R}}(t) = g(t - lT)e^{j\frac{2\pi}{T}k(t - \frac{\alpha T}{2})} \\ g_{k,l}^{\mathcal{I}}(t) = jg(t - lT + T/2)e^{j\frac{2\pi}{T}k(t - \frac{\alpha T}{2})} \end{cases}$$

where, T is symbol period, $K \in \mathbb{N}$ is number of subcarrier, $\alpha \in [0, M - 1]$, and $k, l \in \mathbb{Z}$. The parameter α allows a flexible choice of the center of symmetry of the pulse shaping filter $g(t)$. From the Gabor theory, \mathbf{G} forms a Riesz basis for a separable Hilbert space. For data to be transmitted and received perfectly, in the absence of channel, it is not necessary for the set \mathbf{G} to be orthogonal. In the case it is, the system is called OFDM/OQAM. For any Riesz basis \mathbf{G} , there exists unique dual Riesz basis \mathbf{W} , such that \mathbf{G} and \mathbf{W} are biorthogonal. \mathbf{W} also consist of the pairs of translations and modulations of a some real receiver pulse shape $w(t)$:

$$\mathbf{W} = \begin{cases} w_{k,l}^{\mathcal{R}}(t) = w(t - lT)e^{-j\frac{2\pi}{T}k(t - \frac{\alpha T}{2})} \\ w_{k,l}^{\mathcal{I}}(t) = w(t - lT + T/2)e^{-j\frac{2\pi}{T}k(t - \frac{\alpha T}{2})} \end{cases}$$

where, $k, l \in \mathbb{Z}$.

\mathbf{G} and \mathbf{W} are biorthogonal iff:

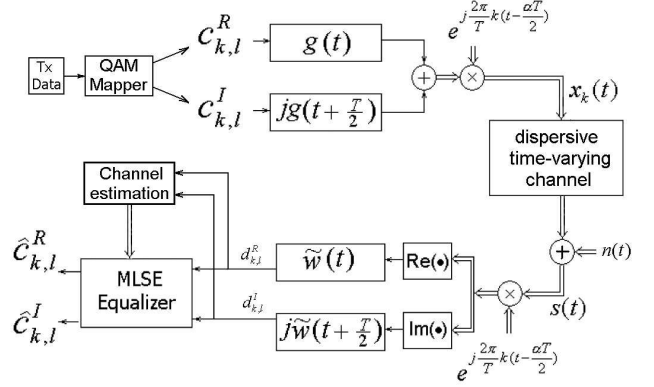


Fig. 1. BFDMM/OQAM system, $\tilde{w}(t) = w(-t)$

$$\Re\{\langle g_{k,l}^{\mathcal{R}}(t), w_{k',l'}^{\mathcal{R}}(t) \rangle\} = \delta_{k,k'} \delta_{l,l'} \quad (5)$$

$$\Im\{\langle g_{k,l}^{\mathcal{R}}(t), w_{k',l'}^{\mathcal{I}}(t) \rangle\} = 0 \quad (6)$$

$$\Re\{\langle g_{k,l}^{\mathcal{I}}(t), w_{k',l'}^{\mathcal{R}}(t) \rangle\} = 0 \quad (7)$$

$$\Im\{\langle g_{k,l}^{\mathcal{I}}(t), w_{k',l'}^{\mathcal{I}}(t) \rangle\} = \delta_{k,k'} \delta_{l,l'} \quad (8)$$

where, $\langle \cdot \rangle$ denotes \mathbf{L}^2 space inner product, $\Re\{\cdot\}$ and $\Im\{\cdot\}$ denote real and imaginary part, respectively, $\delta_{k,k'}$ denotes the Kronecker delta, $k, l, k', l' \in \mathbb{Z}$. For mathematically more thorough discussion on this topic we refer to [3].

B. BFDMM/OQAM SIGNALS

The baseband BFDMM/OQAM signal can be expressed as:

$$x(t) = \sum_{k=0}^{K-1} x_k(t) = \sum_{k=0}^{K-1} \sum_{l=-\infty}^{\infty} \{c_{k,l}^{\mathcal{R}} g_{k,l}^{\mathcal{R}}(t) + c_{k,l}^{\mathcal{I}} g_{k,l}^{\mathcal{I}}(t)\} \quad (9)$$

where, T is symbol period, $c_{k,l}^{\mathcal{R}}, c_{k,l}^{\mathcal{I}}$ are real and imaginary parts of the transmitted symbols $c_{k,l}$, respectively. We assume that $c_{k,l}$ are independent identically distributed (*i.i.d*) random variables. Transmitted signal propagates through mobile multipath channel described in Section II. Received noisy signal may be written as:

$$s(t) = \sqrt{E_s} \sum_m h_m x(t - \tau_m) e^{j2\pi f_m t + \phi_m} + n(t) \quad (10)$$

where E_s is signal energy per channel use, $f_m = f_d \cos \theta_m$ is the Doppler shift of the m -th path, $n(t)$ is additive white Gaussian noise (AWGN) within signal bandwidth with variance $N_0/2$ per complex dimension.

Demodulation performed at the receiver can be expressed as:

$$d_{k',l'}^{\mathcal{R}} = \Re\{\langle s(t), w_{k',l'}^{\mathcal{R}}(t) \rangle\} = \quad (11)$$

$$= \int_{-\infty}^{\infty} \Re\left\{s(\tau) e^{-j\frac{2\pi}{T}k'(\tau - \frac{\alpha T}{2})}\right\} w(\tau - l'T) d\tau$$

$$d_{k',l'}^{\mathcal{I}} = \Im\{\langle s(t), w_{k',l'}^{\mathcal{I}}(t) \rangle\} = \quad (12)$$

$$= \int_{-\infty}^{\infty} \Im\left\{s(\tau) e^{-j\frac{2\pi}{T}k'(\tau - \frac{\alpha T}{2})}\right\} w(\tau + \frac{T}{2} - l'T) d\tau$$

where, $d_{k',l'}^{\mathcal{R}}, d_{k',l'}^{\mathcal{I}}$ are, respectively, the real and imaginary parts of received symbols $d_{k',l'}$. Block diagram of the BFDN/OQAM system is shown in Fig.1. $\tilde{w}(t) = w(-t)$ can be seen as a matched filter to transmitter filter $g(t)$.

C. CHANNEL PARAMETER STATISTICS

Passing through the time-frequency dispersive channel, the transmitted signal loses its biorthogonality causing ISI/ICI at the receiver. Therefore, received symbols in (11) and (12) may be rewritten as:

$$d_{k',l'}^{\mathcal{I}} = \sum_{k,l} \left\{ H_{k,l,\mathcal{R}}^{k',l',\mathcal{I}} c_{k,l}^{\mathcal{R}} + H_{k,l,\mathcal{I}}^{k',l',\mathcal{I}} c_{k,l}^{\mathcal{I}} \right\} + n_{k',l'}^{\mathcal{I}} \quad (13)$$

$$d_{k',l'}^{\mathcal{R}} = \sum_{k,l} \left\{ H_{k,l,\mathcal{R}}^{k',l',\mathcal{R}} c_{k,l}^{\mathcal{R}} + H_{k,l,\mathcal{I}}^{k',l',\mathcal{R}} c_{k,l}^{\mathcal{I}} \right\} + n_{k',l'}^{\mathcal{R}} \quad (14)$$

where, $n_{k',l'}^{\mathcal{I}} = \Im\{\langle n(t), w_{k',l'}^{\mathcal{I}}(t) \rangle\}$ and $n_{k',l'}^{\mathcal{R}} = \Re\{\langle n(t), w_{k',l'}^{\mathcal{R}}(t) \rangle\}$ are noise components. It is easy to check that these are zero-mean Gaussian random variables, $H_{k,l,\mathcal{I}}^{k',l',\mathcal{I}}$, $H_{k,l,\mathcal{R}}^{k',l',\mathcal{I}}$, $H_{k,l,\mathcal{I}}^{k',l',\mathcal{R}}$ and $H_{k,l,\mathcal{R}}^{k',l',\mathcal{R}}$ are the *channel parameters*. In this context, we use a word channel meaning that it includes transmitter and receiver filters, as well as the physical medium. Except the case $k \neq k'$ and $l \neq l'$ they show ISI/ICI caused by the channel. Note that even when $k = k'$ and $l = l'$, $H_{k',l',\mathcal{I}}^{k',l',\mathcal{I}}$ and $H_{k',l',\mathcal{R}}^{k',l',\mathcal{R}}$ show an interference between real and imaginary part of the same symbol. Using (9)-(12) we have:

$$H_{k,l,\mathcal{R}}^{k',l',\mathcal{R}} = \sqrt{E_s} \int_{-\infty}^{\infty} \Re \left\{ \sum_m h_m g(t - lT - \tau_m) \cdot e^{j\frac{2\pi}{T}k(t-\tau_m-\frac{\alpha T}{2M})} e^{j2\pi f_m t + \phi_m} e^{-j\frac{2\pi}{T}k'(t-\frac{\alpha T}{2M})} \right\} \cdot w(t - l'T) dt \quad (15)$$

$$H_{k,l,\mathcal{I}}^{k',l',\mathcal{I}} = \sqrt{E_s} \int_{-\infty}^{\infty} \Im \left\{ \sum_m h_m g(t - lT - \tau_m) \cdot e^{j\frac{2\pi}{T}k(t-\tau_m-\frac{\alpha T}{2M})} e^{j2\pi f_m t + \phi_m} e^{-j\frac{2\pi}{T}k'(t-\frac{\alpha T}{2M})} \right\} \cdot w(t + \frac{T}{2} - l'T) dt \quad (16)$$

$H_{k',l',\mathcal{I}}^{k',l',\mathcal{I}}$ and $H_{k',l',\mathcal{R}}^{k',l',\mathcal{R}}$ can be expressed in the same way. When there large number of paths we may assume that these channel parameters are Gaussian. Therefore, they can be fully described by their first-order and second-order statistics. In this paper we analytically derive these statistics. Using *Assumption I* in Section II, we can rewrite (15) and (16) as:

$$H_{k,l,\mathcal{R}}^{k',l',\mathcal{R}} = \sqrt{E_s} \int_{-\infty}^{\infty} dt \int_0^{\infty} d\tau \Re \{ h(\tau) g(t - lT - \tau_m) \cdot e^{j\frac{2\pi}{T}k(t-\tau_m-\frac{\alpha T}{2M})} \xi(t) e^{-j\frac{2\pi}{T}k'(t-\frac{\alpha T}{2M})} \} w(t - l'T) \quad (17)$$

$$H_{k,l,\mathcal{I}}^{k',l',\mathcal{I}} = \sqrt{E_s} \int_{-\infty}^{\infty} dt \int_0^{\infty} d\tau \Im \{ h(\tau) g(t - lT - \tau_m) \cdot e^{j\frac{2\pi}{T}k(t-\tau_m-\frac{\alpha T}{2M})} \xi(t) e^{-j\frac{2\pi}{T}k'(t-\frac{\alpha T}{2M})} \} w(t + \frac{T}{2} - l'T) \quad (18)$$

Notice that $h(\tau)$ and $\xi(t)$ are statistically independent random processes. Therefore, it can easily be observed that mean

values of channel parameters are zero. Thus, the channel parameters are zero-mean complex Gaussian random variables. Second order statistics can be derived using (2), (4) as:

$$\begin{aligned} \mathbf{E}\{H_{k,l,\mathcal{R}}^{k',l',\mathcal{R}} H_{\tilde{k},\tilde{l},\mathcal{R}}^{k',l',\mathcal{R}}\} &= 2 \int_0^{\infty} d\tau \frac{e^{-\tau/\tau_0}}{\tau_0} \iint_{-\infty}^{\infty} dt_1 dt_2 \\ &\cdot J_0(2\pi f_d | t_1 - t_2 |) g(t_1 - (l - l')T - \tau) w(t_1) \\ &\cdot \cos \left[\frac{2\pi}{T} \left\{ (k - k')(t_1 - \frac{\alpha T}{2N}) - (\tilde{k} - k')(t_2 - \frac{\alpha T}{2N}) - \right. \right. \\ &\quad \left. \left. - (k - \tilde{k})\tau \right\} \right] g(t_2 - (\tilde{l} - l')T - \tau) w(t_2) \quad (19) \end{aligned}$$

$$\begin{aligned} \mathbf{E}\{H_{k,l,\mathcal{R}}^{k',l',\mathcal{R}} H_{\tilde{k},\tilde{l},\mathcal{I}}^{k',l',\mathcal{I}}\} &= 2 \int_0^{\infty} d\tau \frac{e^{-\tau/\tau_0}}{\tau_0} \iint_{-\infty}^{\infty} dt_1 dt_2 \\ &\cdot J_0(2\pi f_d | t_1 - t_2 |) g(t_1 - (l - l')T - \tau) w(t_1) \\ &\cdot \sin \left[\frac{2\pi}{T} \left\{ (\tilde{k} - k')(t_2 - \frac{\alpha T}{2N}) - (k - k')(t_1 - \frac{\alpha T}{2N}) - \right. \right. \\ &\quad \left. \left. - (\tilde{k} - k)\tau \right\} \right] g(t_2 - (\tilde{l} - l')T - \tau) w(t_2 + \frac{T}{2}) \quad (20) \end{aligned}$$

In the same way second-order statistics can be derived for all of the other channel parameters. In Section V, we evaluate these statistics numerically for some practical cases and compare them with the results of computer simulation.

Lastly, we derive autocorrelation and crosscorrelation between noise components. It is easy to check that:

$$\begin{aligned} \mathbf{E}(n_{k,l}^{\mathcal{R}} n_{k',l'}^{\mathcal{R}}) &= \frac{N_O}{2} \int_{-\infty}^{\infty} dt w(t) \\ &\cos \left(\frac{2\pi}{T} (k' - k) (t - \frac{\alpha T}{2K}) \right) \cdot w(t - (l - l')T) \quad (21) \end{aligned}$$

$$\begin{aligned} \mathbf{E}(n_{k,l}^{\mathcal{I}} n_{k',l'}^{\mathcal{I}}) &= \frac{N_O}{2} \cos(\pi(k - k')) \int_{-\infty}^{\infty} dt w(t) \\ &\cdot \cos \left(\frac{2\pi}{T} (k' - k) (t - \frac{\alpha T}{2K}) \right) w(t - (l - l')T) \quad (22) \end{aligned}$$

$$\begin{aligned} \mathbf{E}(n_{k,l}^{\mathcal{I}} n_{k',l'}^{\mathcal{R}}) &= \frac{N_O}{2} \int_{-\infty}^{\infty} dt w(t) \\ &\cdot \sin \left(\frac{2\pi}{T} (k' - k) (t - \frac{\alpha T}{2K}) \right) w(t - (l - l')T + T/2) \quad (23) \end{aligned}$$

Thus, noise components have autocorrelation. The reason is that set \mathbf{W} is not orthogonal. It is easy to observe that crosscorrelation (23) is almost zero. This is because a term inside integration in (23) is odd with respect its center of symmetry.

IV. DESIGN OF BFDN/OQAM SYSTEM

Use of a transmitter pulses that well-localized in time domain as well as in frequency domain, is critically important for OFDM/BFDN system in multipath time-varying channels. One interesting point in BFDN/OQAM is that any symmetric pulse $g(t)$ forms Riesz basis \mathbf{G} , i.e. in the absence of the channel perfect reconstruction of the transmitted symbol is possible with arbitrarily symmetric pulse $g(t)$. In the following subsections we explain the choice of Gaussian transmitter pulse, the Discrete Zak Transform (DZT) and design biorthogonal receiver pulse.

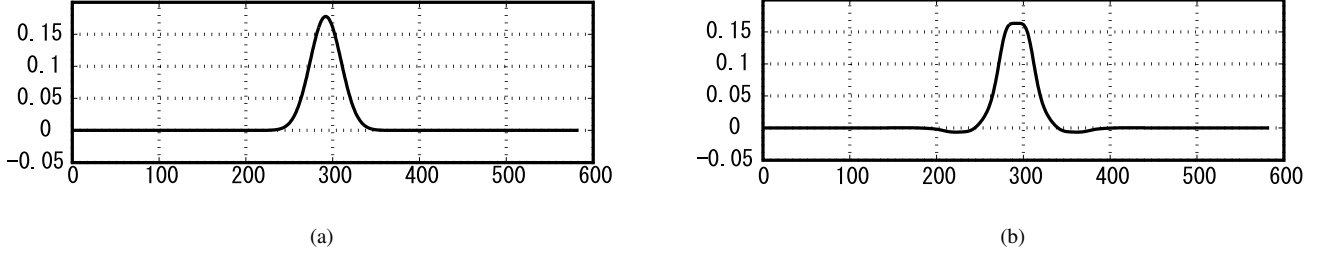


Fig. 2. BFDMM/OQAM biorthogonal pulses, subcarrier number is $K = 64$ and filter length is $L_g = 583$: (a) transmitter pulse, (b) receiver pulse

A. TFL and Gaussian pulse

It is well known that Gaussian pulse has a optimum time-frequency localization (TFL). Classical way to measure the TFL involves Weyl-Heisenberg inequality [4]. More precisely, if $f(t) \in L_2(\mathbb{R})$ and $\tau, \omega \in (\mathbb{R})$ are arbitrary and $\hat{f}(\nu)$ is Fourier transform of $f(t)$ then

$$\left(\int_{-\infty}^{\infty} (t - \tau)^2 |f(t)|^2 dt \right)^{1/2} \times \left(\int_{-\infty}^{\infty} (\nu - \omega)^2 |\hat{f}(\nu)|^2 d\nu \right)^{1/2} \geq \frac{\|f\|^2}{4\pi} \quad (24)$$

where, $\|f\| = (\int |f(t)|^2 dt)^{1/2}$ is L^2 -norm. Equality holds iff $g(t) = ce^{j2\pi\omega(t-\tau)}e^{-\pi\beta(t-\tau)^2}$ for $\tau, \omega \in \mathbb{R}$, $c \neq 0$, and $\beta > 0$, i.e. iff $g(t)$ is translated and modulated Gaussian. In the numerical study in Section V, we consider Gaussian pulse as transmitter $g(t)$ pulse. More detail discussion on pulses with optimal TFL for OFDM/BFDMM systems can be found on [8].

B. DZT AND DESIGN OF BIORTHOGONAL PULSE

Receiver pulse $w(t)$ that is biorthogonal to $g(t)$ pulse can be derived from biorthogonality conditions (5)-(8). For the matter of convenience we consider discrete-time model. (5)-(8) may be rewritten as [5]:

$$\sum_{n=-\infty}^{\infty} g[n - lK]w[n] \cos\left(\frac{2\pi}{K}k(n - \alpha/2)\right) = \delta[l]\delta[k] \quad (25)$$

$$\sum_{n=-\infty}^{\infty} g[n + K/2 - lK]w[n] \sin\left(\frac{2\pi}{K}k(n - \alpha/2)\right) = 0 \quad (26)$$

$$\sum_{n=-\infty}^{\infty} g[n - lK]w[n + K/2] \cos\left(\frac{2\pi}{K}k(n - \alpha/2)\right) = 0 \quad (27)$$

$$\sum_{n=-\infty}^{\infty} g[n + K/2 - lK]w[n + K/2] \cos\left(\frac{2\pi}{K}k(n - \alpha/2)\right) = \delta[l]\delta[k] \quad (28)$$

where, $g[n] = g(nT/K)$ and $n \in \mathbb{Z}$. If $g[n]$ is supported in $[0, L_g - 1]$, we observe that choosing $\alpha = (L_g + K/2 - 1) \bmod K$, even functions $g[n]$ and $w[n]$ with the same symmetry $g[n] = g[\alpha + (2r + 1)K/2 - n]$ would satisfy (26),

(27). In the design of biorthogonal pulse we need Discrete-Time Zak transform (DZT) [9] of the pulse $g[n]$, which is defined as:

$$\mathcal{Z}_g^{(K/2)}(n, \theta) = \sum_{r=-\infty}^{\infty} g\left[n + r\frac{M}{2}\right] e^{-j2\pi r\theta} \quad (29)$$

Inverse can be found as:

$$g[n] = \int_0^1 \mathcal{Z}_g^{(M/2)}(n, \theta) d\theta \quad (30)$$

Then applying DZT to (25) or (28) we have [5]:

$$\mathcal{Z}_g^{(K/2)}(n, \theta) \mathcal{Z}_w^{(K/2)*}(n, \theta) + \mathcal{Z}_g^{(K/2)}(n, \theta - 1/2) \mathcal{Z}_w^{(K/2)*}(n, \theta - 1/2) = \frac{4}{K} \quad (31)$$

If $g[n]$ is supported in $[0, L_g - 1]$, we observe that choosing $\alpha = (L_g + K/2 - 1) \bmod M$, even functions $g[n]$ and $w[n]$ with the same symmetry, that expressed as:

$$g[n] = g[\alpha + (2r + 1)K/2 - n] \quad (32)$$

would satisfy (26) and (27). Indeed, it can be shown that these pulses would also satisfy (31). It follows from (31) and (32) that:

$$\mathcal{Z}_w^{(K/2)}(n, \theta) = \frac{4\mathcal{Z}_g^{(K/2)}(n, \theta)}{K \left\{ |\mathcal{Z}_g^{(K/2)}(n, \theta)|^2 + |\mathcal{Z}_g^{(K/2)}(n, \theta - 1/2)|^2 + \right\}} \quad (33)$$

The biorthogonal pulse employed by transmitter and receiver filters, in a numerical example and simulation, is shown in Fig.2. (a) and (b).

V. NUMERICAL STUDY AND DISCUSSION

In this section we first, simulate BFDMM/OQAM system and derive second-order channel statistics. Second, we numerically evaluate analytic formulae (19)-(20) for second-order statistics, and compare the results with those derived by simulation.

We consider BFDMM/OQAM signal with $K = 64$ subchannels, digital modulation uses 16QAM. Transmitter filter uses Gaussian pulse Fig.2 (a). Biorthogonal pulse for receiver filter is generated using (33) and shown on Fig.2 (b). Filter length is $L_g = 583$.

In computer simulation, the channel parameter statistics are approximated by generating at least 500 independent samples

of the channel parameters and averaging them. Simulation is conducted on a fixed value $k' = 30$ and $l' = 0$. The simulation channel has exponentially decaying delay profile with rms delay spread $\tau_0 \in [0.1\mu s, 1\mu s]$, and Jakes' Doppler Power spectrum with maximum Doppler shift $f_d \in [70Hz, 700Hz]$, which corresponds to vehicle speed of $v \in [30km/h, 300km/h]$, at carrier frequency $f_c = 2.5GHz$. Complex amplitudes of each path are zero-mean Gaussian random variables with variance defined in (1). Symbol period of the system is set to match the channel, i.e. $T = 840\mu s \approx \sqrt{(\tau_0/f_d)}$.

In numerical evaluation, the channel parameter statistics are calculated using formula (19), with the same parameters used in computer simulation.

Figure 3 (a) and (b) show autocorrelation $\mathbf{E}\{H_{k,l,\mathcal{R}}^{30,0,\mathcal{R}^2}\}$ vs. subcarrier separation k , at different values of the maximum Doppler shift, i.e. speed of vehicle. The former is generated by numerical evaluation of (19), and the latter is by computer simulation. We observe that the results are almost the same. Autocorrelation take local minimum values at even numbers of frequency separation. On the other hand, Fig.3 (c) and (d) plot $\mathbf{E}\{H_{k,l,\mathcal{R}}^{30,0,\mathcal{R}^2}\}$ at different values of rms delay spread τ_0 . As previous, (c) is derived by numerically evaluation of (19), and (d) is by computer simulation. At practical values of τ_0 the results are the same. However at $\tau_0 = 0.1\mu s$ the result from computer simulation shows sharp drops at even number of frequency separation. It is also of interest to plot autocorrelation vs. time separation. In Fig. 3. (e) and (f) $\mathbf{E}\{H_{k,l,\mathcal{R}}^{30,0,\mathcal{R}^2}\}$ is plotted vs. time separation, by numerical evaluation of (19). The former plots at different values of vehicle speed, and latter plots at different values of τ_0 . We observe that the relation is log-linear.

VI. CONCLUSIONS

In this paper we studied ISI/ICI, channel parameters and their second-order statistics for BFDN/OQAM system in time-frequency dispersive channel. We derived analytical equation for second-order channel statistics and numerically evaluated them and compared with the results obtained by computer simulation. We have observed that these two values are almost the same for the practical cases.

REFERENCES

- [1] Y. Li, L. J. Cimini, N. R. Sollenberger, "Robust Channel Estimation for OFDM Systems with Rapid Dispersive Fading Channels," IEEE Trans. on Comm., vol. 46, No 7, pp. 902-914, Jul. 1998.
- [2] P. K. Remvik, N. Holte, and A. Vahlin, "Fading and carrier frequency offset robustness for different pulse shaping filters in OFDM" Vehicular Technology Conference, 1998. vol 2, pp. 777 - 781, May 1998
- [3] H. G. Feichtinger and T. Strohmer, "Gabor Analysis and Algorithms: Theory and Applications," Boston, MA: Birkhäuser, 1998.
- [4] T. Strohmer and S. Beaver, "Optimal OFDM Design for Time-Frequency Dispersive Channels," IEEE Trans. on Comm., vol. 51, No 7, pp. 1111-1122, Jul. 2003.
- [5] H. Bölcskei, "Orthogonal frequency division multiplexing based on offset QAM," in *Advances in Gabor Analysis*, H. G. Feichtinger and T. Strohmer, Boston, MA: Birkhäuser, 2002.

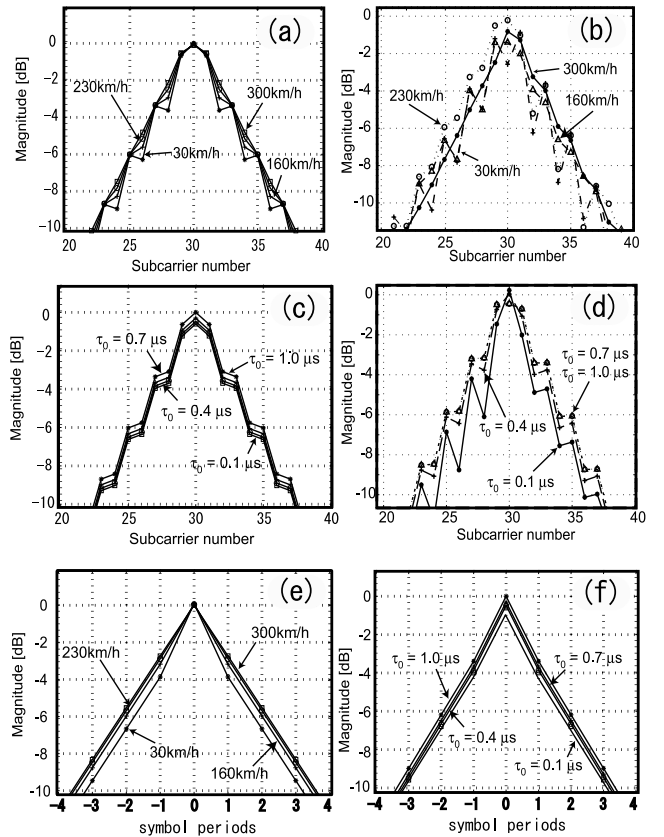


Fig. 3. Channel parameter statistics, $\mathbf{E}\{H_{k,l,\mathcal{R}}^{30,0,\mathcal{R}^2}\}$, (a) obtained by evaluating formula (19), at different values of vehicle speed, (b) obtained by simulation, at different values of vehicle speed, (c) obtained by evaluating formula (19), at different values of τ_0 , (d) obtained by simulation, at different values of τ_0 , (e) vs. time separation, at different values of vehicle speed, by formula (19), (f) vs. time separation, at different values of τ_0 , by formula (19).

- [6] D. Schfbuber, G. Matz and F. Hlawatsch, "Pulse-Shaping OFDM/BFDN Systems for Time-Varying Channels: ISI/ICI Analysis, Optimal Pulse Design, and Efficient Implementation," PIMRC 2002, vol 3, pp. 1012 - 1016, 2002.
- [7] W. C. Jakes, *Microwave Mobile Communications*. Piscataway, NJ: IEEE Press, 1994.
- [8] H. Bölcskei and A.J. E. M. Janssen, "Gabor frames, unimodularity and window decay," J.Four. Anal.Appl., vol 6 pp. 255-276, 2000.
- [9] H. Bölcskei and F. Hlawatsch, "Discrete Zak transforms, polyphase transforms, and applications," IEEE Trans. Sig. Proc., vol 45, pp. 851-866, April 1997.

ACKNOWLEDGMENTS

This work was supported in part by the The 21st Century COE Program by the Ministry of Education, Culture, Sports, Science and Technology in Japan, and Fujitsu Laboratory.